



Potential Roles of Serum Exosomal CD155 and its Impact on NK Cell Immunosuppression in Hepatocellular Carcinoma

Wenzheng Han^{1, #}, Jinrong Lv^{2, #}, Mintuo Wang^{1, #}, Xiaoxin Wu³, Dongdong Sun¹, Wenwen Chen², Yingying Wang¹, Wenjie Zhou¹, Yuxuan Yang¹, Jia Bao¹, Qingzhen Han⁴, Xiaopeng Chen¹, Fei Guo⁵, Gang Feng¹, Min Li², Qing Chen¹

¹The First Affiliated Hospital, Wannan Medical College, Anhui, China

²Institute of Biology and Medical Sciences, Soochow University, Jiangsu, China

³State Key Laboratory for Diagnosis and Treatment of Infectious Diseases, National Clinical Research Centre for Infectious Diseases, The First Affiliated Hospital, Zhejiang University School of Medicine, Zhejiang, China

⁴Center of Clinical Laboratory and Translational Medicine, The Fourth Affiliated Hospital of Soochow University, Suzhou Dushu Lake Hospital, Suzhou, Jiangsu, China

⁵Department of Urology, Changhai Hospital, Naval Medical University, Shanghai, China

#These authors contributed equally to this work.

Background: Targeted therapies directed at tumor immune checkpoint, like programmed death-ligand (PD-L)1/programmed death (PD)-1, have shown remarkable progress. Nevertheless, treatment efficacy in hepatocellular carcinoma (HCC) is notably compromised due to the intricate immune microenvironment. Exploring alternative checkpoints beyond PD-L1/PD-1, including those not located on the cell surface, may improve our understanding of their roles in areas like diagnostic potential and immune tolerance in HCC.

Aims: To explore the roles of serum exosomal CD155 (exo-CD155) in HCC.

Study Design: Experimental study.

Methods: We separated and analyzed serum exosomes from HCC patients. We quantified the concentrations of serum soluble CD155 (sCD155) and serum exo-CD155, and examined their association with disease progression, hepatitis B surface antigen (HBsAg) presence, and the concentrations of α -fetoprotein fraction L3 (AFP-L3) or alpha-fetoprotein

(AFP). Additionally, we assessed the diagnostic effect through the receiver operating characteristic (ROC) curve, and the immune suppressive effect on natural killer (NK) cells of exo-CD155.

Results: This study reveal elevated exo-CD155 levels in all HCC patients, with a significant increase in early-stage patients, exhibiting normal AFP/AFP-L3 or HBsAg-positive status. Exo-CD155 is linked to the progression of HCC and shows significant diagnostic effectiveness for the disease. Furthermore, the incubation of NK-92MI with exosomes derived from HCC patients leads to a substantial reduction in immune function, which can be partially counteracted with an antibody that blocks T cell immune receptor immunoglobulin and ITIM domains, (TIGIT)-blocking antibody.

Conclusion: These results disclose exo-CD155 shows promise for serving as a biomarker for HCC, especially in early-stage patients or those with normal AFP/AFP-L3 levels. Moreover, serum exosomes from HCC patients suppress NK cell immune functions through the TIGIT/CD155 pathway, contributing to immune tolerance in HCC.

INTRODUCTION

The manipulation of immune checkpoints has arisen as a fundamental cornerstone in cancer immunotherapy, focusing on unleashing immune responses against tumors. Strategies such as checkpoint blockade have transformed the therapeutic field of

multiple tumors, notably non-small cell lung cancer and melanoma.¹ Nonetheless, the application in hepatocellular carcinoma (HCC) presents challenges in attaining optimal therapeutic outcomes.^{2,3} The upregulation of diverse immune checkpoint expressions serves as a strategic mechanism adopted by HCC to evade immune surveillance,



Corresponding author: Qing Chen, The First Affiliated Hospital, Wannan Medical College, Anhui, China

e-mail: chenq1104@wnmc.edu.cn

Received: January 31, 2025 **Accepted:** April 17, 2025 **Available Online Date:** May 05, 2025 • **DOI:** 10.4274/balkanmedj.galenos.2025.2025-1-129

Available at www.balkanmedicaljournal.org

ORCID iDs of the authors: W.H. 0009-0009-2175-5107; J.L. 0009-0000-5770-9596; M.W. 0009-0002-5109-9154; X.W. 0000-0001-9785-8916; D.S. 0000-0002-5182-4398; W.C. 0009-0002-1076-1623; Y.W. 0009-0008-6243-2091; W.Z. 0009-0003-9665-8885; Y.Y. 0009-0000-1502-7909; J.B. 0009-0004-3480-7379; Q.H. 0000-0001-7373-891X; X.C. 0000-0002-3087-5735; F.G. 0009-0004-2149-7228; G.F. 0000-0002-8378-8248; M.L. 0009-0005-5993-9084; Q.C. 0009-0004-4308-3990.

Cite this article as: Han W, Lv J, Wang M, Wu X, Sun D, Chen W, Wang Y, Zhou W, Yang Y, Bao J, Han Q, Chen X, Guo F, Feng G, Li M, Chen Q. Potential Roles of Serum Exosomal CD155 and its Impact on NK Cell Immunosuppression in Hepatocellular Carcinoma. *Balkan Med J.*; 2025; 42(3):242-53.

Copyright@Author(s) - Available online at <http://balkanmedicaljournal.org/>

thus substantially impeding the effectiveness of anti-programmed-death ligand (PD-L)1/programmed death (PD)-1 treatment.^{4,5} Consequently, it is crucial to explore mechanisms associated with alternative immune checkpoints in hepatocarcinogenesis to improve the effectiveness of HCC treatment.

Initially found to be a receptor for poliovirus, CD155 is now known to be a type I transmembrane glycoprotein belonging to the immunoglobulin superfamily. Notably, its expression is minimal or absent in normal tissue cells. Tumor cells often exhibit aberrantly elevated levels of CD155 expression.^{6,7} CD155 exerts a critical function in tumor immune escape, as cancer cells have the ability to diminish the immune effectiveness of effector cells through membranous CD155 (mCD155).^{8,9} CD155 serves as the ligand for both co-stimulatory receptors (like CD226) and co-inhibitory receptors, such as the T cell immune receptor with immunoglobulin and ITIM domains, (TIGIT), on T cells and natural killer (NK) cells. Notably, the strength of CD155's binding to TIGIT significantly exceeds its binding to CD226.¹⁰ Studies have reported that inhibiting the interaction of CD155 with TIGIT prevents the dysfunction of NK cells, and elicited a robust immune response against tumors.^{11,12} Furthermore, aside from mCD155, soluble CD155 (sCD155) in serum is markedly elevated in cancer patients, suggesting its promise as a valuable indicator for tumor detection and prognosis. In 2021, Zhang et al.¹³ reported a recombinant oncolytic adenovirus that expressing sCD155 triggered prolonged anti-tumor immune surveillance. Beyond CD155, NK cells, within the intricate and dynamic tumor microenvironment of HCC patients, often exhibit compromised functionality, leading to reduced antitumor activity. This impairment is characterized by a decrease in the expression of critical molecules such as Siglec-7, alongside an upsurge in the concentrations of checkpoint molecules including TIGIT and PD-L1.¹⁴⁻¹⁶

Exosomes are vesicles, ranging from 30 to 150 nm, enclosed by membranes found outside the cell. They are crucial for cell-to-cell interaction, as they can influence the functions and behaviors of the cells receiving their cargo.^{17,18} Exosomes originating from cancer cells are termed tumor-derived exosomes (TEXs). TEXs are pivotal to the immune escape of HCC and affect the function of NK cells through various mechanisms.¹⁹ Zhang et al.²⁰ uncovered that circUHRF1 carried by exosomes, originating from tumors, induces exhaustion in NK cells and could lead to failure of anti-PD1 treatment in HCC. TEXs inhibit NK cells by transferring molecules like transforming growth factor- β and microRNA (miR)-23a.²¹ Chen et al.²² documented that an elevated amount of exosomal PD-L1 was released from metastatic melanoma, suggesting its expression as a predictor for anti-PD-1 treatment. Poggio et al.²³ observed that PD-L1 that is carried by exosomes could effectively curb anti-tumor immune function and memory. However, although these studies have reported the significant role of PD-L1-expressing TEXs (exosomal PD-L1) in cancer patients, it remains unclear whether TEXs from HCC patients carry CD155. Therefore, identifying the level of checkpoint molecules (especially CD155) on TEXs, as well as revealing their impact on NK cells, may hold substantial clinical application value. Additionally, assuming that TEXs do carry CD155, it is still unknown whether the level of exosomal CD155 (exo-CD155) correlates with tumor progression and whether they can induce

tumor immunosuppression through their action on NK cells in HCC.

Moreover, it is well established that the principal predisposing factor for HCC is chronic hepatitis B virus (HBV) infection, particularly in endemic regions. Hepatitis B surface antigen (HBsAg) serves as a key indicator for assessing HBV infection in patients.^{24,25} However, to date, there are no reports documenting the distinguishing expression of exo-CD155 in HCC patients who are either HBsAg-positive or HBsAg-negative. Some studies have also noted that a number of HCC patients present with normal α -fetoprotein fraction L3 (AFP-L3) and/or alpha-fetoprotein (AFP) levels, thereby limiting the ability to diagnose HCC based on these marker measurements.^{26,27} This study examines if exo-CD155 shows significant alterations in these HCC patients.

In our study, we aimed to investigate the expression of CD155 on serum exosomes and explore its correlation with HCC across different stages, varying HBsAg statuses, and diverse AFP or AFP-L3 levels. Additionally, we assessed the diagnostic efficiency of exo-CD155 as well as its immunosuppressive effects on NK cells in the context of HCC.

MATERIALS AND METHODS

Subjects

The study recruited patients fulfilling these criteria: HCC diagnosis confirmed through histopathology, imaging, and/or laboratory tests; availability of peripheral blood sampling collection in a fasting state for analysis; no prior anticancer therapies, including chemotherapy, radiotherapy, or targeted therapy; and no record of familial cancers or concurrent cancers. The exclusion criteria included other malignant tumors, combined liver metastases, use of immunomodulatory medication within the past six months, and severe autoimmune diseases or psychiatric disorders. We selected subjects as healthy controls (HC) who underwent routine health check-ups during the same timeframe, and whose results confirmed liver health, without a history of liver diseases. These participants had not been subjected to treatments or medications that could impact liver health, nor did they have any significant or chronic illnesses. Their liver function indicators were required to be within normal limits, encompassing but not limited to aspartate aminotransferase, total bilirubin, and alanine aminotransferase levels. The medical features of subjects were shown in Table 1. The study was approved by the Ethics Review Committee of the First Affiliated Hospital of Wannan Medical College (approval no: 202167, date: 08.03.2021), and the experimental procedures conformed to the Declaration of Helsinki. Written informed consent was obtained from all subjects.

Materials

For our study, we employed the NK-92MI cell line-genetically modified, infinitely proliferative NK cells originating from lymphoma patients-to examine the roles of exo-CD155 on NK cell immune response *in vitro*. We also used the K562 cell line, a type of granulocytic leukemia cell with infinite proliferative capacity derived from leukemia patients, as target cells to assess

the cytotoxic capability of NK cells *in vitro*. Both cell lines were obtained from Procell Co., Ltd. (Wuhan, China). Table 2 lists the key antibodies, the assay kits, and their corresponding suppliers. The isotype-matched immunoglobulin G (IgG) antibodies used as controls for flow cytometric analysis were all procured from BioLegend [CA, United State of America (USA)]. Recombinant

interleukin (IL)-15 protein of human origin was acquired from PeproTech (Cranbury, NJ, USA).

Isolation and characterization of exosomes

Serum exosomes were obtained using an exosome extraction reagent kit following the manufacturer's protocol. Briefly, the

TABLE 1. Clinical Features of the Enrolled Subjects.

Variable	HCC (n = 82)	HC (n = 59)	p value
Age (year)	64.5 ± 11.0	61.4 ± 8.0	> 0.05
Gender (M/F)	64 (78.0%)/18 (22.0%)	45/14	> 0.05
HBsAg status (-/+)	36 (43.9%)/46 (56.1%)	Negative	
Cirrhosis, n (%)	82 (100%)	0 (0%)	
Clinical stage (I/II/III/IV)	40 (48.8%)/10 (12.2%)/23 (28.0%)/9 (11.0%)	NM	
Lymph node metastasis (-/+)	54 (65.9%)/28 (34.1%)	NM	
Extrahepatic metastasis (-/+)	66 (80.5%)/16 (19.5%)	NM	
Microvascular invasion (-/+)	61 (74.4%)/21 (25.6%)	NM	
Child-Pugh (A/B/C)	70 (85.4%)/11 (13.4%) /1 (1.2%)	NM	
WHO grade (1/2/3)	37 (45.1%)/34 (41.5%) /11 (13.4%)	NM	
AFP (ng/mL)	191.8 (6.0, 1664.4)	NM	
AFP-L3 (ng/mL)	7.9 (0.3, 262.0)	NM	

Values are presented as mean ± SD, median (P25, P75), number, and/or percentage. (-/+), negative/positive. Barcelona Clinic Liver Cancer (BCLC) staging system for clinical stage. The differentiation degree of HCC can be classified into three grades- well-differentiated (grade 1), moderately differentiated (grade 2), and poorly differentiated (grade 3)-according to the WHO 2019 edition
HCC, hepatocellular carcinoma; HC, healthy control; M/F, male/female; AFP, alpha-fetoprotein; AFP-L3, alpha-fetoprotein heterogeneity-L3; NM, not measured; SD, standard deviation; WHO, World Health Organization

TABLE 2. Key Antibodies or Kit Used in the Experiments.

Catalog No.	Supplier	Antibody/kit
ab275377	Abcam	Recombinant Anti-ALIX antibody [EPR23653-32]
ab8219	Abcam	Anti-CD63 antibody [MEM-259]
317333	Biolegend	PE/Cyanine7 anti-CD3 Antibody (OKT3)
362545	Biolegend	FITC anti-CD56 (NCAM) Antibody (5.1H11)
372207	Biolegend	PE anti-Granzyme B Antibody (QA16A02)
372705	Biolegend	APC anti-TIGIT Antibody (A15153G)
812545	CST	PVR/CD155 (D8A5G) Rabbit mAb
ab125011	Abcam	Anti-TSG101 antibody [EPR7130(B)]
M20006S	Abmart	GAPDH (3B3) Mouse mAb
GC68355	GlpBio	Tiragolumab (Anti-TIGIT)
ZWK132	ZWK Medical Technology	Anti-human CD56 antibody [MyM1-123C3]
ZWK133	ZWK Medical Technology	Anti-human TIGIT antibody [MyR1-BLR047F]
2530-CD/CF	RD	Recombinant Human CD155/PVR
DY285B-05	RD Systems	Human IFN-γ ELISA kit
DY210-05	RD Systems	Human TNF-α ELISA kit
C0037	Beyotime	Cell Counting Kit-8
G1780	Promega	CytoTox 96® Non-Radioactive Cytotoxicity Assay
C1272-10	Applygen	Exosome Extraction Reagent kit
23225	Thermo Scientific	BCA Protein Assay kit

serum sample was thawed at 37 °C, centrifuged for 20 min at 2000 g, and the collected supernatant underwent centrifuge further at 10000 g for 20 min to remove cell debris. The second supernatant was transferred into a tube containing the exosome extraction reagent, and the tube was incubated at 4 °C for 2 hours while being shaken vigorously. Further spinning at 1500g for 15 min, yielded the precipitates, which contained the serum exosomes. Phosphate buffered saline (PBS) was employed to reconstitute serum exosomes which were stored along with the exosome-free serum at -20 °C until use. Exosomal morphology was detected by transmission electron microscopy (TEM), and the size dispersion profile of the exosomes was examined using nanoparticle tracking analysis (NTA). Expression of Alix and CD63 on the exosomes was detected using western blot. Glyceraldehyde-3-phosphate dehydrogenase (GAPDH) was employed as the control.

Western blot

Proteins extracted from the serum exosomes with radioimmunoprecipitation assay (RIPA) buffer, were quantified with the bicinchoninic acid (BCA) protein assay kit. The proteins isolated on sodium dodecyl sulfate polyacrylamide gel electrophoresis (SDSPAGE) gel were transferred to a polyvinylidene difluoride membrane and blocked with 5% skimmed milk powder. Following washing, the membrane was exposed to the diluted primary antibodies [Alix (1:2000), CD63 (1:2000), CD155 (1:1000), TSG-101 (1:1000), and GAPDH (1:1000)], subsequently treated with horseradish peroxidase (HRP)-labeled secondary antibodies (anti-rabbit (1:8000) and goat anti-mouse (1:8000) antibodies), and finally washed with phosphate buffered saline with Tween-20 (PBST). The immunoreactive bands were visualized with GAPDH expression as the control.

Flow cytometry

Separation of human peripheral blood mononuclear cells (PBMCs) was carried out using samples from HCC patients and HC subjects through Ficoll-Paque density gradient centrifugation at 1200g for 30 min, and then redispersed in Roswell Park Memorial Institute Medium 1640. After the antibodies (anti-CD3, anti-CD56, anti-TIGIT) were added to the prepared PBMCs, examination of the cells was performed using a fluorescence-activated cell sorting Verse analyzer (BD, CA, USA). To detect the level of intracellular granzyme B (GrB), NK-92MI cells were exposed to IL-15 (5 ng/mL) with or without serum exosomes (10 µg/mL) in the presence or absence of the anti-TIGIT antibody (20 µg/mL) for 24 h. After adding Brefeldin A (BFA) (5 µg/mL), NK-92MI were cultured for 4 more hours, and then collected by spinning at 1500g for 10 minutes. They were prepared for analysis by fixing, permeabilizing, and staining with anti-GrB antibody before being analyzed. Isotype-matched IgG antibodies were used in all procedures.

Cell proliferation assay

NK-92MI cells were plated and exposed to IL-15 (5 ng/mL) under conditions with or without serum exosomes (10 µg/mL) obtained from subjects with or without the anti-TIGIT antibody (20 µg/mL) for

24 h. The premixed cell counting kit-8 was subsequently transferred to each well and incubated for 60 minutes at 37 °C; afterwards, the optical density (OD) at 450 nm was examined.

Cytotoxicity assay

To investigate the destructive impact of NK cells on K562 cells, the lactate dehydrogenase (LDH) release cytotoxicity assay was employed. NK-92MI cells underwent pre-activation with IL-15 (5 ng/mL), supplemented with either serum exosomes (5 or 10 µg/mL) the anti-TIGIT antibody (20 µg/mL), both, or neither, and then exposed to K562 for 4 hours at an effector-to-target ratio of 10:1. Lysis percentage was calculated using the non-radioactive cytotoxicity assay kit as follows:

$$X = [(A-B-C)/(D-C)] * 100\%$$

where X is the percent cytotoxicity, A is the experimental LDH release, B represents the baseline LDH release from the effector cell, C indicates the spontaneous LDH release of the target cell, and D is the highest level of LDH release obtained from the target cell. The OD was measured at 490 nm.

Immunohistochemistry (IHC)

The paraffin-embedded specimens were dewaxed, and heat-induced antigen retrieval was performed. After blocking the endogenous peroxidase with 0.3% hydrogen peroxide and 3% bovine serum albumin, the specimens were exposed to primary antibodies for TIGIT (1:100) and CD56 (1:100) for 24 hours at 4 °C. They were subsequently exposed to the HRP-labeled secondary antibody (1:4000) for 30 minutes at room temperature. TIGIT and CD56 expression levels were revealed through staining with diaminobenzidine tetrahydrochloride (Zhongshan Golden Bridge Biotechnology, China). The slides were counterstained with hematoxylin for 5 min in a room temperature environment, then inspected under an optical microscope at the high-power field. Images were taken for five randomly chosen spots.

Enzyme-linked immunosorbent assay (ELISA)

The concentrations of interferon (IFN)-γ and tumor necrosis factor (TNF)-α from the supernatant of cell culture along with sCD155 and exo-CD155 levels, were quantified using ELISA as described below. The cell culture supernatant for TNF-α and IFN-γ detection, 100 µL of exosome-free serum, and serum exosomes derived from 100 µL of serum samples from each HCC patient or HC subject for sCD155 and exo-CD155 detection, and standard samples were specifically transferred into 96-well plates previously prepared with the corresponding antibodies. These plates were then cultured at 4 °C overnight. The plates underwent four washes with PBST, were incubated with HRPlabeled antibodies at room temperature for 60 min, and were thereafter subjected to four PBST washes. After the addition of 3,3',5,5'-tetramethylbenzidine as the chromogenic substrate, the plates were incubated in darkness at room temperature for 20 min before the absorbance (450 nm) were measured by microplate reader (ThermoFisher Scientific Inc., MA, USA).

Statistical analysis

SPSS 22.0 software (SPSS Inc., IL, USA) was used to evaluate the data. The χ^2 test was used to compare the genders of two groups. We applied the Shapiro-Wilk test to assess whether the data conformed to a normal distribution. The comparison between two independent cohorts used the Mann-Whitney U test (non-parametric test) or Student's t-test (parametric test) where appropriate. For datasets that followed a normal distribution, we conducted a one-way ANOVA to compare three or more groups, followed by Tukey's Honest Significant Difference test as a post-hoc analysis to determine the corrected significance of pairwise comparisons. For data that did not meet the assumption of normal distribution, we opted for the Kruskal-Wallis test to compare three or more groups, and used Dunn's test for post-hoc analysis to determine the corrected significance of pairwise comparisons. Pearson correlation analysis was used where applicable. G*Power software 3.1.9.7 (Heinrich-Heine-Universität Düsseldorf, Germany) was used as a tool for statistical power analysis. The diagnostic efficiencies of exo-CD155 were examined by employing the receiver operating characteristic (ROC) curves. The criterion for statistical significance in all tests was set at $p < 0.05$, with all tests being two-tailed.

RESULTS

Clinical features of the subjects

Eighty-two patients with HCC, and 59 HC were enrolled, and the detailed medical features were presented in Table 1. Of the 82 HCC patients, 46 (56.1%) were HBsAg-positive. The HCC patients were categorized based on histopathological evaluations and the Barcelona Clinic Liver Cancer staging system into stages I/II/III/IV (40/10/23/9 patients).²⁸ Briefly, in our study, stage I represents very early (0) or early (A) stage; stage II represents intermediate stage (B); stage III represents advanced stage (C); stage IV represents terminal stage (D). Among the patients, 28 (34.1%) exhibited lymph node metastasis, 16 (19.5%) showed extrahepatic metastasis, and 21 (25.6%) demonstrated microvascular invasion. There were 37 (45.1%) patients with well-differentiated, 34 (41.5%) with moderately differentiated, and 11 (13.4%) with poorly differentiated HCC.²⁹ Notably, all patients had underlying cirrhosis.³⁰ According to the Child-Pugh classification, the distribution was as follows: 70 patients (85.4%) were classified as Class A, 11 patients (13.4%) as Class B, and 1 patient (1.2%) as Class C. The median serum AFP level was 191.8 ng/mL (P25, 6.0 ng/mL; P75, 1664.4 ng/mL), and the median value of AFP-L3 was found to be 7.9 ng/mL (P25, 0.3 ng/mL; P75, 262.0 ng/mL).

Extraction and characterization of serum exosomes

Serum exosomes were effectively isolated and purified from all subjects, as demonstrated in Figure 1a. TEM revealed typical exosomal morphology (Figure 1b), while NTA showed an average diameter of 112.5 ± 37.5 nm (Figure 1c). The measurement of markers CD63 and Alix carried by exosomes was verified by western blot analysis, while GAPDH detected in PBMCs served as a control (Figure 1d).

Elevated serum exosomal CD155 levels in advanced HCC patients

Serum concentrations of exo-CD155 and sCD155 were quantified using a CD155 ELISA kit. Both exo-CD155 and sCD155 concentrations were markedly elevated in HCC patients compared with HC subjects (Figure 2a, b). Notably, exo-CD155 levels were substantially higher than sCD155 levels in HCC patients at both early (stage I + II) and advanced (stage III + IV) stages (Figure 2c, d). Further investigation revealed that sCD155 levels differed significantly only between stage I + II patients with HCC and HC subjects (Figure 2e), while exo-CD155 levels followed the pattern: stage III + IV > stage I + II > HC subjects (Figure 2f). sCD155 levels differed significantly only between stage-I patients with HCC and HC subjects (Figure 2g), while exo-CD155 was markedly elevated in stage I, III, and IV patients with HCC compared to HC subjects (Figure 2h). Moreover, HCC patients with lymph node or extrahepatic metastasis showed significantly higher exo-CD155 levels, compared to sCD155 levels, than those without metastasis (Figure 2i, j), indicating a strong correlation between exo-CD155 and advanced HCC.

Higher exosomal CD155 levels in HBsAg-positive HCC patients

Exosomal and soluble CD155 levels were analyzed in stage I + II HCC patients based on their HBsAg status. While no obvious difference in sCD155 levels was found between patients with positive HBsAg and those with negative HBsAg (Figure 3a), exo-CD155 levels demonstrated a significant elevation in HBsAg-positive patients (Figure 3b). In contrast, neither sCD155 nor exo-CD155 levels exhibited any remarkable differences among stage III + IV patients based on HBsAg status (Figure 3c, d). These results suggest that exo-CD155, rather than sCD155, is closely associated with HBsAg-positive status in early-stage HCC patients.

Elevated exosomal CD155 levels in both AFP/AFP-L3-positive and -negative HCC patients

To investigate whether the exo-CD155 levels or sCD155 levels were associated with the AFP/AFP-L3 status in HCC patients, the levels of exo-CD155 and sCD155 in the stage I + II HCC patients based on their AFP or AFP-L3 status were analyzed. sCD155 levels were significantly higher only in AFP-negative or AFP-L3-negative patients with HCC compared to HC subjects (Figure 4a, c). Conversely, exo-CD155 levels were consistently elevated in stage I + II HCC patients compared to HC subjects, irrespective of their AFP or AFP-L3 status (Figure 4b, d). Among stage III + IV HCC patients, sCD155 levels were indistinguishable between groups (Figure 4e, g), while exo-CD155 levels remained elevated regardless of AFP or AFP-L3 status (Figure 4f, g). These observations imply that serum exo-CD155 is a robust marker for HCC, regardless of AFP/AFP-L3 status.

Diagnostic values of exo-CD155 for patients with HCC

Considering the promising diagnostic indicator of exo-CD155 in HCC, we undertook an analysis of its diagnostic efficacy. ROC curve of exo-CD155 (area under the curve = 0.843; $p < 0.0001$) demonstrated significant diagnostic efficiency for HCC (Figure 5). The cutoff value of 4737.8 pg/mL in exo-CD155 had a sensitivity of 64.9% and specificity of 98.1% for the diagnosis of HCC.

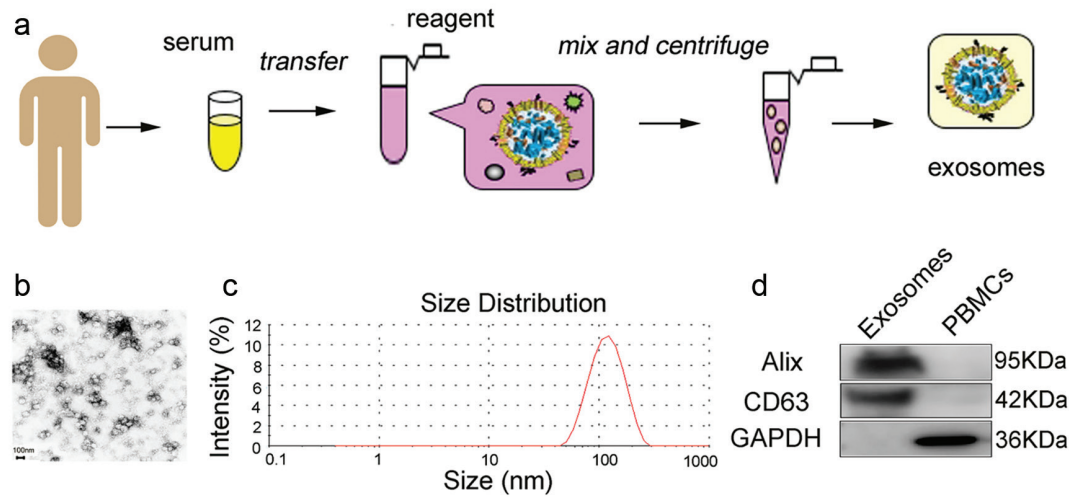


FIG. 1. Isolation and characterization of exosomes from HCC patients and HC subjects. (a) The flowchart delineating the procedure for obtaining serum exosomes. (b,c) Transmission electron microscopy (TEM) and nanoparticle tracking analysis (NTA) were utilized to assess the morphology and size distribution of the exosomes. (d) The expression of Alix and CD63 on the exosomes was examined via Western blot, with GAPDH used as the control. All tests were conducted in triplicate.

HCC, hepatocellular carcinoma; HC, healthy controls.

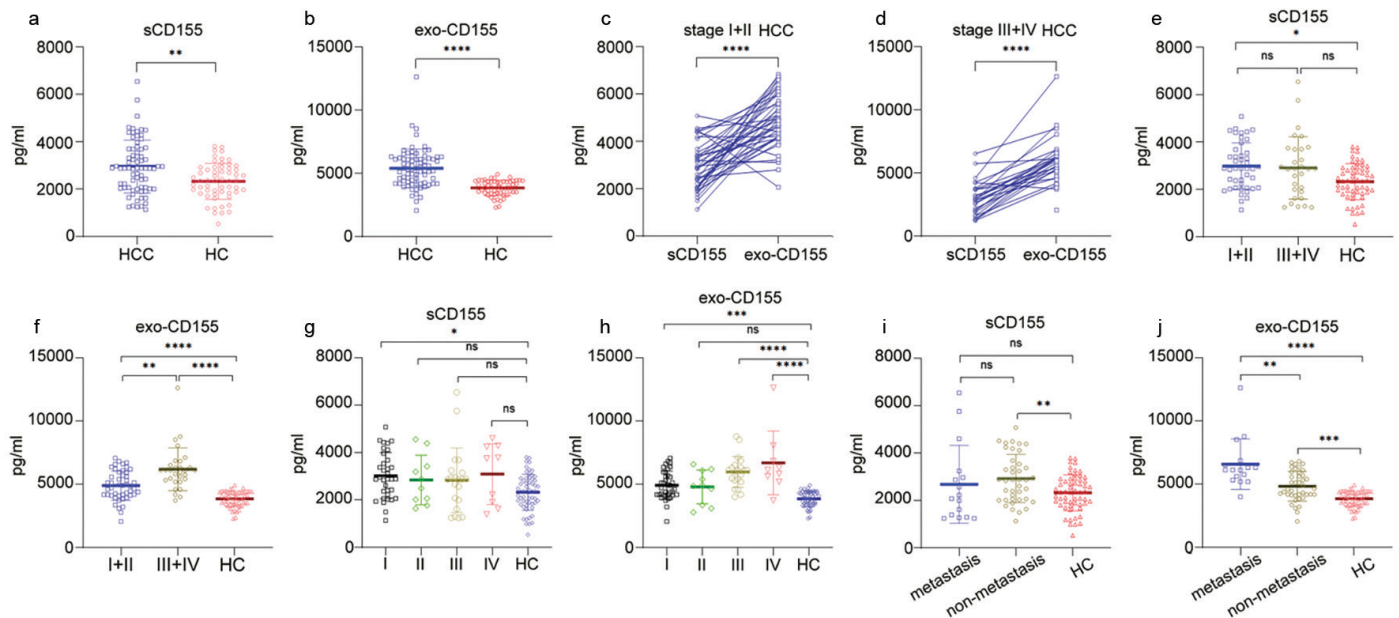


FIG. 2. Expression levels of sCD155 and exo-CD155 in HCC patients and HC subjects. (a, b) The levels of sCD155 and exo-CD155 were detected and analyzed in HCC patients and HC subjects, as well as (E-H) in HCC patients at different stages. (c, d) sCD155 and exo-CD155 levels in each HCC patient at stage I + II or III + IV were examined and assessed. (i, j) The levels of sCD155 or exo-CD155 among patients with or without metastasis and HC groups were measured and analyzed. Data are represented as mean \pm SD. HCC, hepatocellular carcinoma; HC, healthy control. * $p < 0.05$; ** $p < 0.01$; *** $p < 0.001$; **** $p < 0.0001$; ns = not significant. Mann-Whitney U test, One-way ANOVA followed by Tukey's Honest Significant Difference as a post-hoc test to determine the corrected significance of pairwise comparisons, or Kruskal-Wallis test followed by Dunn's test as a post-hoc test to ascertain the corrected significance of pairwise comparisons was used where appropriate.

SD, standard deviation.

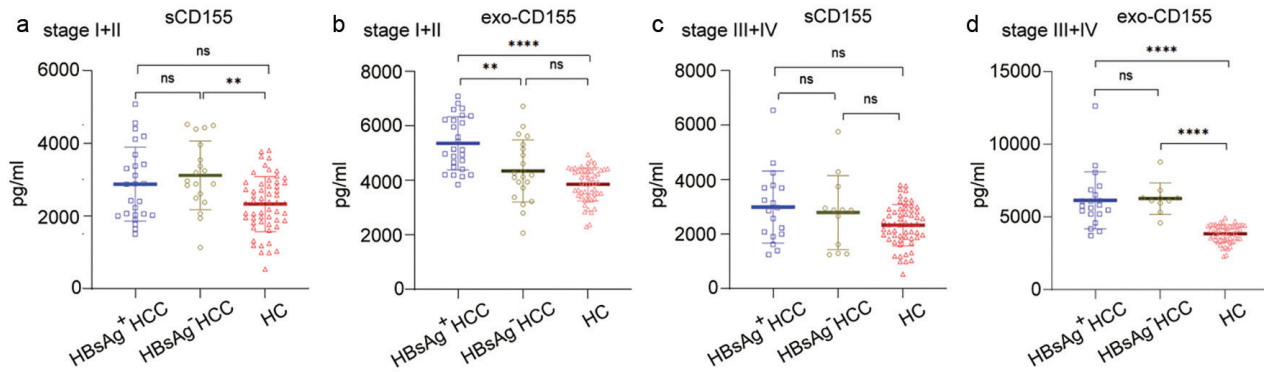


FIG. 3. Expression levels of sCD155 and exo-CD155 in HCC patients with different HBsAg status. The levels of sCD155 and exo-CD155 were analyzed in (a, b) stage I + II and (c, d) stage III + IV HCC patients divided by their HBsAg status. Data are represented as mean ± SD. HCC, hepatocellular carcinoma; HC, healthy control. ** $p < 0.01$; **** $p < 0.0001$; ns = not significant.

SD, standard deviation; HBsAg, hepatitis B surface antigen.

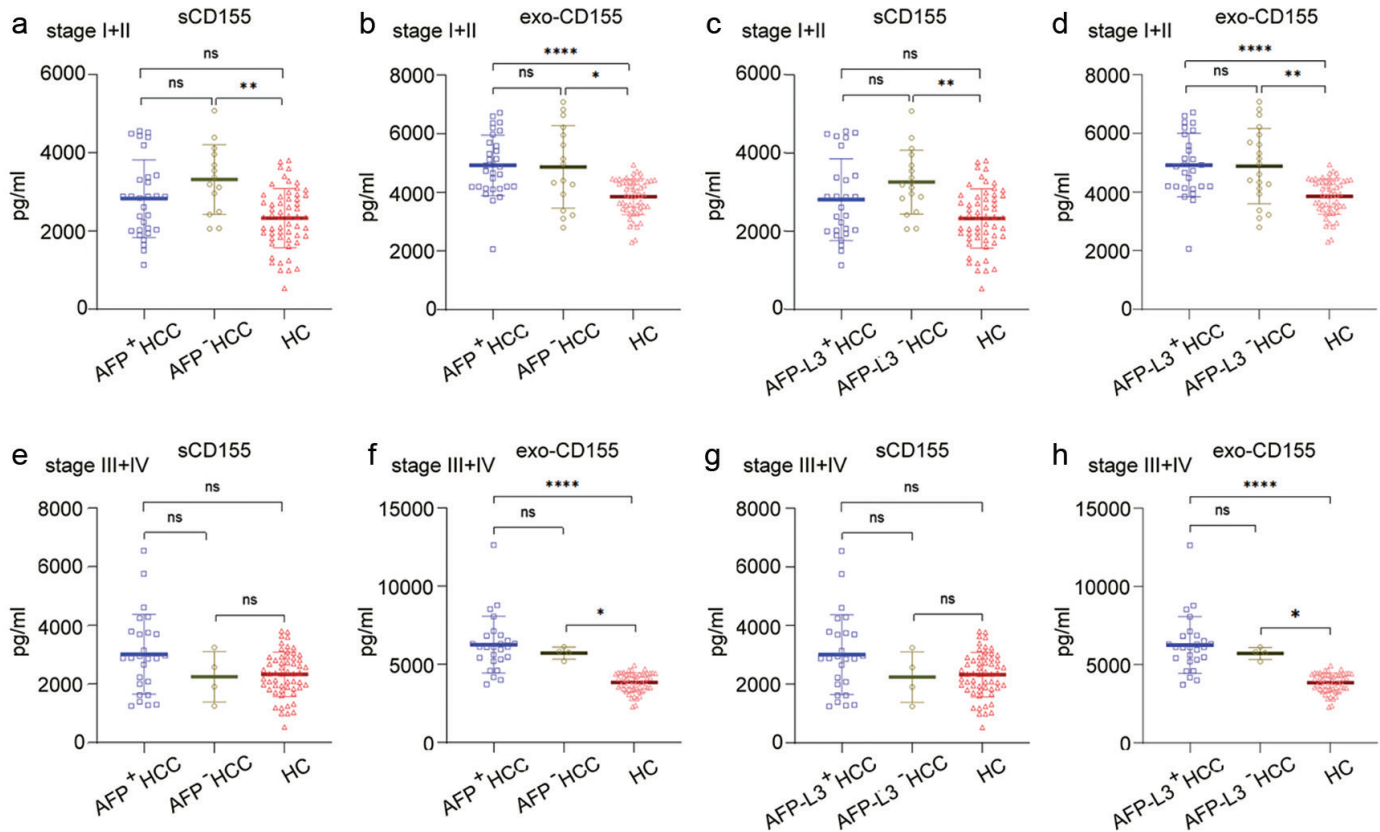


FIG. 4. Expression levels of sCD155 and exo-CD155 in HCC patients with different AFP or AFP-L3 status. The levels of sCD155 and exo-CD155 were analyzed in stage I + II HCC patients with different (a, b) AFP and (c, d) AFP-L3 status. The expression levels of sCD155 and exo-CD155, were analyzed in stage III + IV HCC patients with different (e, f) AFP and (g, h) AFP-L3 status. Data are represented as mean ± SD. HCC, hepatocellular carcinoma; HC, healthy control. * $p < 0.05$; ** $p < 0.01$; **** $p < 0.0001$; ns = not significant.

SD, standard deviation.

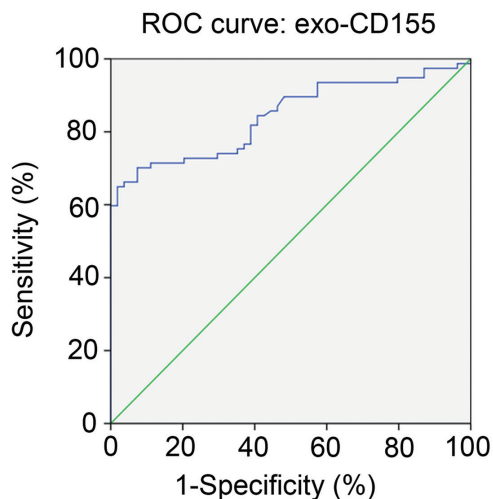


FIG. 5. Diagnostic efficiency of exo-CD155. The ROC curve was employed to assess the diagnostic efficiency of exo-CD155 for patients with HCC.

ROC, receiver operating characteristic curve; HCC, hepatocellular carcinoma.

Increased expression of TIGIT on NK cells in advanced HCC patients

TIGIT expression on NK cells was remarkably elevated in stage III + IV HCC patients in comparison with stage I + II patients and HC subjects, respectively (Figure 6a, c). A inverse correlation was detected between TIGIT upregulation and the percentage of NK cells in PBMCs (Figure 6d, e). Immunohistochemical staining further confirmed that tumor regions from stage III + IV patients with HCC had the lowest proportions of CD56+ NK and the highest TIGIT expression (Figure 6f, g). Compared to the paracancerous areas (within 2 cm from the tumor edge) in the specimens, the tumor areas of stage I + II HCC patients had a significantly lower quantity number of CD56+ NK cells, but an indistinguishable level of TIGIT expression (Figure 6f, h). These observations indicate that increased TIGIT expressed on NK cells is closely linked to advanced HCC.

Serum exosomes from HCC patients suppress NK cell functions

To explore the effect of serum exosomes on NK cells, NK-92MI was cultured with exosomes from HCC. Exosomes significantly inhibited NK-92MI cell proliferation (Figure 7a) and cytotoxicity toward K562 target cells (Figure 7b). Additionally, exosomes diminished the secretion of IFN- γ , TNF- α (Figure 7c, d), intracellular GrB levels (Figure 7e, f), indicating that exosomes from HCC patients suppress NK cell immune functions.

TIGIT Blockade Restores NK Cell Immune Functions

To assess the function of the CD155/TIGIT pathway in NK suppression, NK-92MI was exposed to an anti-TIGIT blocking antibody. Anti-TIGIT treatment partially restored NK cell proliferation (Figure 8a), cytotoxicity (Figure 8b), and the concentrations of IFN- γ , TNF- α , and GrB (Figure 8c, f) in the presence of exosomes derived from HCC, confirming the role of the CD155/TIGIT axis in immune suppression.

DISCUSSION

Previous studies have shown that sCD155 is linked to various tumor types. Jin et al.³¹ disclosed that the concentrations of sCD155 were significantly elevated in HCC and were closely associated with poor prognosis and an immunosuppressive microenvironment. sCD155 inhibits the cytolytic activity of NK and promotes the malignant progression of melanoma.³² The levels of sCD155 showed a positive association with tumor sizes, tumor stage, and age in breast cancer patients. Furthermore, sCD155 levels were decreased in patients with estrogen receptor (ER)-positive tumors compared to those with ER-negative tumors, and were increased in patients with high Ki-67 expression tumors compared to those with low Ki-67 expression tumors.³³ In our study sCD155 is not effective in differentiating HCC patients at various stages, despite its elevated levels in patients compared to HC subjects. Moreover, in HCC patients with and without metastasis, there is no obvious difference in sCD155 levels. Notably, sCD155 levels were significantly lower than those of exo-CD155 in both early (stage I + II) and advanced (stage III + IV) HCC patients. This indicates that the primary form of CD155 present in early or advanced HCC patients is exosomal rather than soluble. It is well known that exosomes play crucial functions in tumor biology, including diagnosis, treatment, metastasis, prognosis, and immune regulation.³⁴ In the present research, exo-CD155 levels were remarkably elevated in HCC patients at all stages and demonstrated a clear association with disease progression, particularly in distinguishing between early and advanced patients with HCC; they showed significant diagnostic efficiency for HCC. It is important to note that 82 HCC patients and 59 HC subjects were enrolled in our study, with power analysis performed to justify our sample sizes. For the comparison of sCD155 levels between HCC and HC, upon calculation, the effect size of $d = 0.64$ (medium effect size) based on two datasets (including mean, standard deviation, and sample size), using a significance threshold of 0.05 (two-sided). The power analysis using G*Power software indicated a statistical power of 95.11% (power = 0.9511). For the comparison of exo-CD155 levels between HCC and HC, upon calculation, the effect size of $d = 1.26$ (large effect size) based on two datasets. The power analysis indicated a statistical power of 95.15% (power = 0.9515). This result indicates that our study is adequately powered to detect significant differences between the two groups. However, it is important to note that while we did not perform an a priori power analysis, we now report the observed effect sizes. We also acknowledge that future studies should incorporate prospective power calculations based on clinically meaningful differences.

The incidence of HCC is strongly associated with HBV infection,^{35,36} and chronic HBV infection has been linked to elevated levels of both CD155 and TIGIT.^{37,38} In our study, sCD155 levels were not influenced by HBsAg status in HCC patients. However, exo-CD155 levels were notably elevated in HBsAg-positive cases, particularly in those at early disease stages. Specifically, exo-CD155 levels were highest in HBsAg-positive stage I + II patients, followed by HBsAg-negative stage I + II patients, and then HC. These findings indicate that exo-CD155, rather than sCD155, has significant clinical value in diagnosing early-stage HCC with HBV infection.

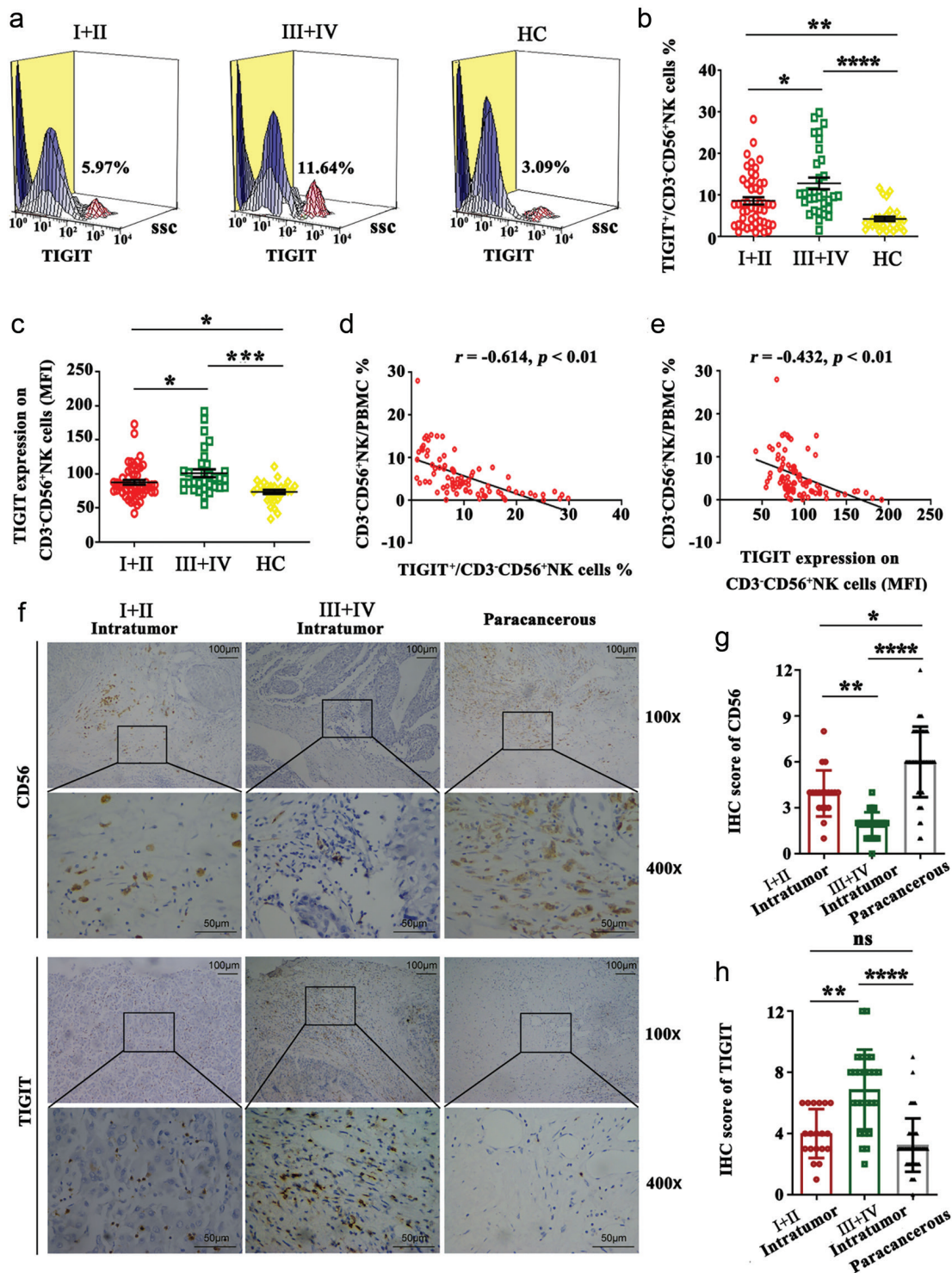


FIG. 6. Correlation between TIGIT expression and the proportion of NK cells in HCC patients. (a) Representative images of the proportions of TIGIT expression on CD3-CD56 + NK cells in HCC patients at different stages and HC subjects were displayed, and (b, c) the proportions and MFI of TIGIT expression were analyzed. (d, e) Correlation analysis between the TIGIT level and the proportion of peripheral CD3-CD56+NK cells. (f) IHC of the paraffin-embedded tumor specimens, and (g, h) IHC scores of the CD56 and TIGIT levels in the respective areas. MFI, median fluorescence intensity. * $p < 0.05$; ** $p < 0.01$; *** $p < 0.001$; **** $p < 0.0001$; ns = not significant.

HCC, hepatocellular carcinoma; HC, healthy controls; IHC, immunohistochemistry; NK, natural killer.

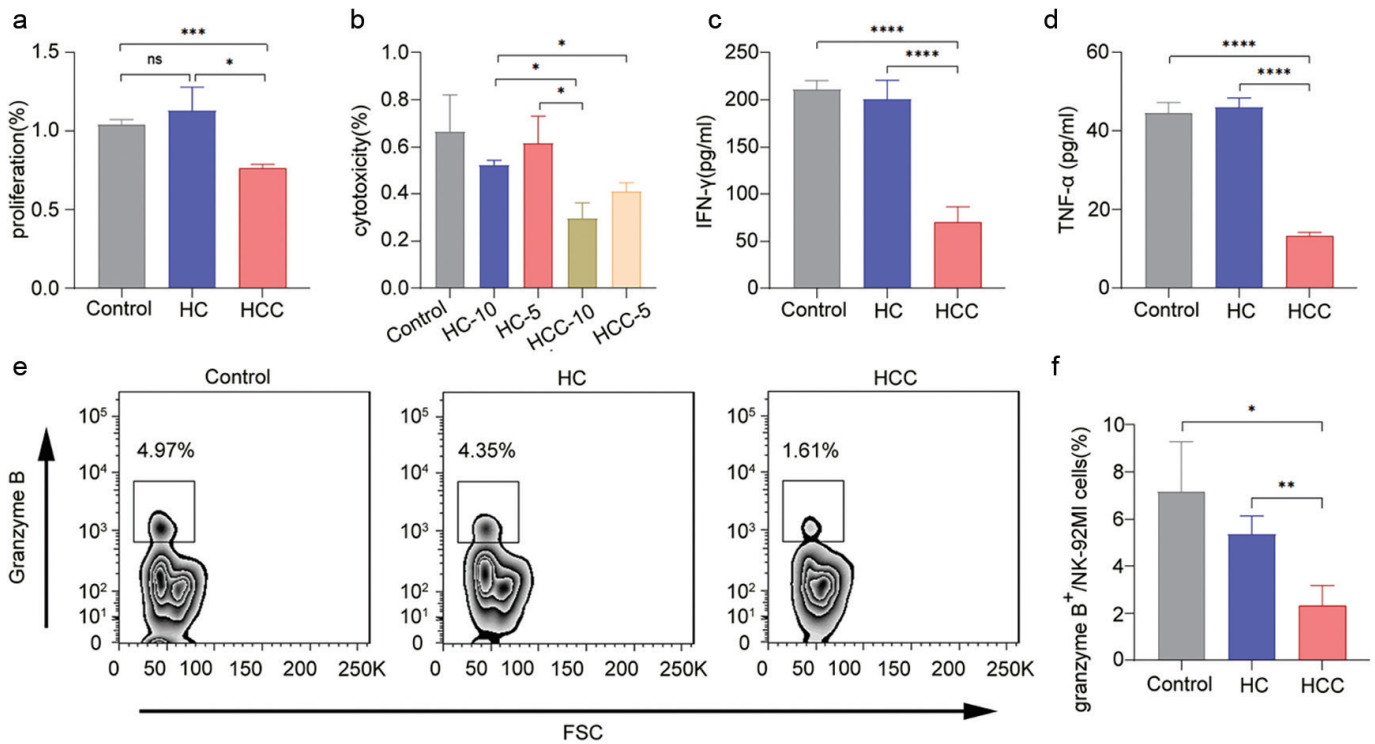


FIG. 7. *In vitro* assessment of the immune functions of NK-92MI cells stimulated by serum exosomes. The NK-92MI cells were incubated with exosomes derived from HCC patients or HC subjects following activation with IL-15. Subsequently, the immune functions of the NK-92MI cells were assessed, including: (a) proliferation, (b) cytotoxicity, (c, d) levels of IFN-γ and TNF-α, and (e, f) levels of granzyme B. * $p < 0.05$; ** $p < 0.01$; *** $p < 0.001$; **** $p < 0.0001$; ns = not significant.

HCC, hepatocellular carcinoma; HC, healthy controls; IL, interleukin; IFN, interferon; TNF, tumor necrosis factor, NK, natural killer.

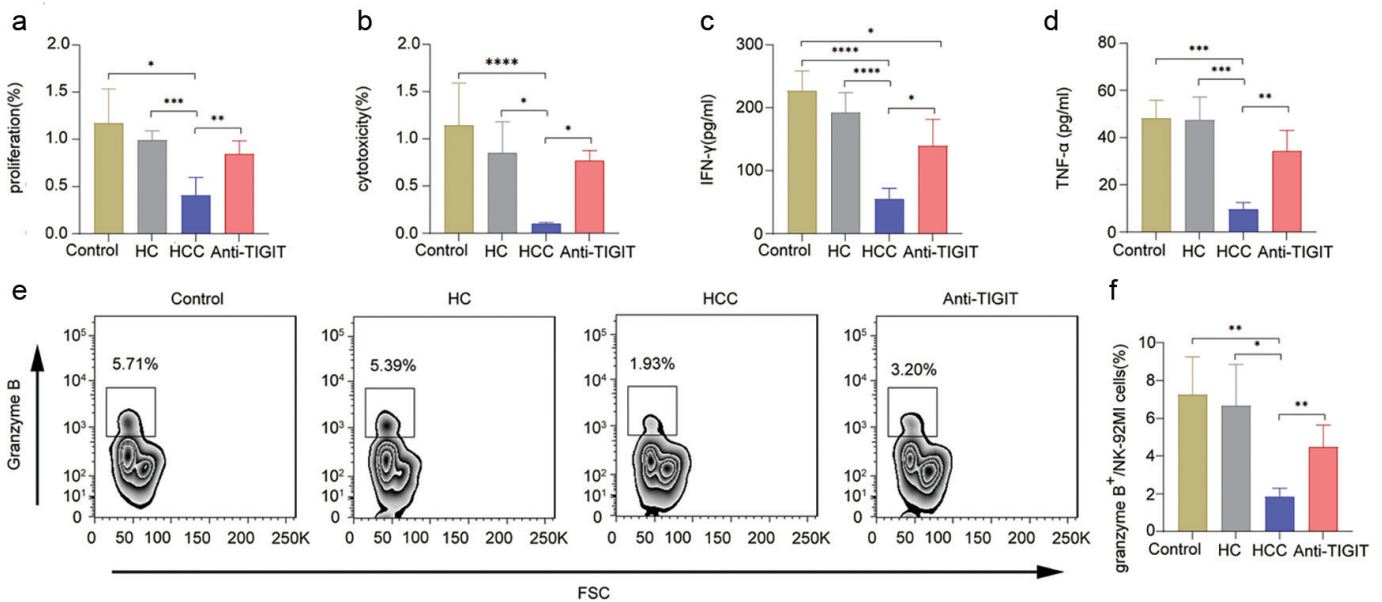


FIG. 8. Reversal of the immune dysfunctions of NK-92MI cells by anti-TIGIT. The NK-92MI cells were incubated with the exosomes originated from HCC patients or HC subjects, following activation with IL-15, with or without anti-TIGIT. And then, the immune functions of NK-92MI cells were examined, including: (a) proliferation, (b) cytotoxicity, (c, d) levels of IFN-γ TNF-α, and (e, f) granzyme B. * $p < 0.05$; ** $p < 0.01$; *** $p < 0.001$; **** $p < 0.0001$.

HCC, hepatocellular carcinoma; HC, healthy controls; IL, interleukin; IFN, interferon; TNF, tumor necrosis factor, NK, natural killer.

In the clinic, AFP and AFP-L3 are widely used as non-invasive biomarkers for HCC diagnosis, however, a substantial subset of patients tests negative for these markers, despite having the disease.³⁹ Other non-invasive biomarkers, such as protein induced by vitamin K absence or antagonist II, miR, and heat shock protein 90a (HSP90a), have been explored to improve HCC diagnosis.³⁹⁻⁴¹ Recently, tumor-originated exosomes have arisen as promising biomarkers for tumor detection and monitoring.^{42,43} In our research, we found that exo-CD155 levels were consistently increased in both early- and advanced-stage HCC patients, regardless of their AFP or AFP-L3 status. This suggests that exo-CD155 could serve as a valuable biomarker, especially for AFP/AFP-L3-negative patients with HCC. Interestingly, while sCD155 was elevated in AFP/AFP-L3-negative patients at early stages, it failed to distinguish between AFP/AFP-L3-positive and negative patients, highlighting the superiority of exo-CD155.

As expected, we observed reduced proportions of NK cells present in the circulating blood of HCC patients, consistent with previous studies showing that NK cell dysfunction is common in HCC.^{44,45} The malfunction of NK cells in HCC can be ascribed to several factors, such as PD-L1/PD-1 signaling, TIGIT upregulation, and the influence of tumor-originated exosomes.⁴⁶⁻⁴⁸ In our study, elevated serum exo-CD155 levels were linked to an obvious reduction in the proportion of NK cells in HCC patients' PBMCs. Additionally, exosomes from HCC significantly impaired NK-92MI cell capabilities, such as cytokine production, cytotoxicity, and proliferation. Importantly, the levels of TIGIT expression had an inverse relationship with NK cell proportions, and blocking the CD155/TIGIT pathway partially restored NK-92MI cell function. Moreover, recombinant CD155 inhibited NK cell immune functions, but this inhibition was reversed to varying degrees upon CD155/TIGIT blockade (Supplementary Figure 1). These findings disclose that HCC-related exosomes suppress NK cell functions through the TIGIT/CD155 axis, contributing to immune tolerance.

However, it is important to acknowledge the challenges associated with culturing primary NK cells *in vitro*, including difficulties in obtaining sufficient quantities and notable variability among cells from different individuals. These challenges prompted us to utilize the NK-92MI cell line for our *in vitro* studies due to its ease of culture, ready access, and high uniformity. It should still be noted that NK-92MI, characterized by specific attributes, cannot entirely mimic primary NK cells. Originating from the circulating blood NK cells of a non-Hodgkin's lymphoma patient, the NK-92MI cell line has been genetically modified (through IL-2 gene transfection) to achieve unlimited proliferation and potent cytotoxic activity, albeit with a narrower killing spectrum. Additionally, these cells lack CD16 molecules, which precludes their engagement in antibody-dependent cellular cytotoxicity for target cell elimination.^{49,50} Considering these characteristics, this study utilized IL-15-stimulated NK-92MI cells for a set of *in vitro* experiments to illuminate the impact of exosomal CD155 on NK-92MI cell functions, including proliferation, cytokine secretion, and K562 cell killing, thereby providing reliable insights into the mechanisms of immune evasion in HCC patients.

In our study, there are several limitations. Firstly, although the research was conducted within a single hospital, the stringent

inclusion criteria and rigorous methodology bolster the reliability of our findings. Recognizing the importance of cohort diversity, we acknowledge the need to expand our study population in future research to enhance the generalizability of our results. To achieve this, we intend to collaborate with additional hospitals to gather a wider array of clinical samples and further substantiate our conclusions. Secondly, given the relatively low incidence of HCC and the intricate process involved in collecting patient data and samples, it was not feasible for us to recruit a sufficient number of participants.

In conclusion, serum exo-CD155 holds potential as a new indicator for HCC, particularly for early-stage patients or those with normal AFP/AFP-L3 levels. Serum exosomes from HCC patients contribute to immune tolerance, in part, through the TIGIT/CD155 pathway.

Acknowledgements: The data analysis, article-editing and revising process, and article submission process received careful and kind guidance from Prof. Jianhua Wang, Fudan University Shanghai Cancer Center.

Ethics Committee Approval: The study was approved by the Ethics Review Committee of the First Affiliated Hospital of Wannan Medical College (approval no: 202167, date: 08.03.2021), and the experimental procedures conformed to the Declaration of Helsinki.

Informed Consent: Written informed consent was obtained from all subjects.

Data Sharing Statement: The datasets analyzed during the current study are available from the corresponding author upon reasonable request.

Authorship Contributions: Concept- X.C., G.F., M.L., Q.C.; Design- W.H., G.F., M.L., Q.C.; Supervision- M.L., Q.C.; Materials- W.Z., Y.Y., J.B.; Data Collection or Processing- W.H., J.L., M.W., X.W., D.S., W.C., Y.W., Q.H.; Analysis and/or Interpretation- W.H., J.L., M.W.; Literature Review- Q.H., F.G. Writing- W.H., M.L.; Critical Review- X.C., G.F.

Conflict of Interest: The authors declare that they have no conflict of interest.

Funding: The present study was supported by the Natural Science Foundation of Universities in Anhui Province (grant no. KJ2021A0835, 2023AH051742, KJ2021ZD0102 and 2024AH051936), the Health Research Foundation of Anhui Province (grant no. AHWJ2023A20546), the National College Students' Innovation and Entrepreneurship Training Program (grant no. 202210368023), the College Students' Innovation and Entrepreneurship Training Program in Anhui Province (grant no. S202310368052, S202310368121 and S202210368049), the National Natural Science Foundation of China (grant no. 82300004), Zhejiang Provincial Natural Science Foundation of China (grant no. LQ21H190004), Natural Science Foundation of Shanghai (grant no. 21ZR1479000), the Rising-Star Program of Shanghai Qihang Program (23QA1411900), and Natural Science Foundation of Wannan Medical College (grant no. WK2023ZZD20).

Supplementary Figure 1: <https://www.balkanmedicaljournal.org/img/files/2025.2025-1-125-supplemantry.pdf>

REFERENCES

1. Shiravand Y, Khodadadi F, Kashani SMA, et al. Immune checkpoint inhibitors in cancer therapy. *Curr Oncol*. 2022;29:3044-3060. [CrossRef]
2. Meng Y, Ye F, Nie P, et al. Immunosuppressive CD10+ALPL+ neutrophils promote resistance to anti-PD-1 therapy in HCC by mediating irreversible exhaustion of T cells. *J Hepatol*. 2023;79:1435-1449. [CrossRef]
3. Li Q, Han J, Yang Y, Chen Y. PD-1/PD-L1 checkpoint inhibitors in advanced hepatocellular carcinoma immunotherapy. *Front Immunol*. 2022;13:1070961. <http://doi.org/10.3389/fimmu.2022.1070961>
4. Leone P, Solimando AG, Fasano R, et al. The evolving role of immune checkpoint inhibitors in hepatocellular carcinoma treatment. *Vaccines (Basel)*. 2021;9:532-550. [CrossRef]
5. Sové RJ, Verma BK, Wang H, Ho WJ, Yarchoan M, Popel AS. Virtual clinical trials of anti-PD-1 and anti-CTLA-4 immunotherapy in advanced hepatocellular carcinoma using a

- quantitative systems pharmacology model. *J Immunother Cancer*. 2022;10:e005414. Erratum in: *J Immunother Cancer*. 2023;11:e005414corr1. [\[CrossRef\]](#)
6. Huang DW, Huang M, Lin XS, Huang Q. CD155 expression and its correlation with clinicopathologic characteristics, angiogenesis, and prognosis in human cholangiocarcinoma. *Oncotargets Ther*. 2017;10:3817-3825. [\[CrossRef\]](#)
 7. Triki H, Charfi S, Bouzidi L, et al. CD155 expression in human breast cancer: Clinical significance and relevance to natural killer cell infiltration. *Life Sci*. 2019;231:116543. [\[CrossRef\]](#)
 8. Liu L, Wang A, Liu X, et al. Blocking TIGIT/CD155 signalling reverses CD8+ T cell exhaustion and enhances the antitumor activity in cervical cancer. *J Transl Med*. 2022;20:280-293. [\[CrossRef\]](#)
 9. He W, Zhang H, Han F, et al. CD155/TIGIT signaling regulates CD8+ T-cell metabolism and promotes tumor progression in human gastric cancer. *Cancer Res*. 2017;77:6375-6388. [\[CrossRef\]](#)
 10. Chauvin JM, Zarour HM. TIGIT in cancer immunotherapy. *J Immunother Cancer*. 2020;8:e000957. [\[CrossRef\]](#)
 11. Wang F, Liu S, Liu F, et al. TIGIT immune checkpoint blockade enhances immunity of human peripheral blood NK cells against castration-resistant prostate cancer. *Cancer Lett*. 2023;568:216300. [\[CrossRef\]](#)
 12. Chauvin JM, Ka M, Pagliano O, et al. IL15 stimulation with TIGIT blockade reverses CD155-mediated NK-Cell dysfunction in melanoma. *Clin Cancer Res*. 2020;26:5520-5533. [\[CrossRef\]](#)
 13. Zhang H, Zhang Y, Dong J, et al. Recombinant oncolytic adenovirus expressing a soluble PVR elicits long-term antitumor immune surveillance. *Mol Ther Oncolytics*. 2020;20:12-22. [\[CrossRef\]](#)
 14. Xiao R, Tian Y, Zhang J, et al. Increased Siglec-9/Siglec-9L interactions on NK cells predict poor HCC prognosis and present a targetable checkpoint for immunotherapy. *J Hepatol*. 2024;80:792-804. [\[CrossRef\]](#)
 15. Yu L, Liu X, Wang X, et al. TIGIT+ TIM-3+ NK cells are correlated with NK cell exhaustion and disease progression in patients with hepatitis B virus related hepatocellular carcinoma. *Oncimmunology*. 2021;10:e1942673. [\[CrossRef\]](#)
 16. Wang K, Gu C, Yu G, et al. Berberine enhances the anti-hepatocellular carcinoma effect of NK92-MI cells through inhibiting IFN-gamma-mediated PD-L1 expression. *Liver Res*. 2022;6:167-174. [\[CrossRef\]](#)
 17. Krylova SV, Feng D. The Machinery of Exosomes: Biogenesis, Release, and Uptake. *Sci Int J Mol Sci*. 2023;24:1337. [\[CrossRef\]](#)
 18. Pegtel DM, Gould SJ. Exosomes. *Annu Rev Biochem*. 2019;88:487-514. [\[CrossRef\]](#)
 19. Han Q, Zhao H, Jiang Y, Yin C, Zhang J. HCC-derived exosomes: critical player and target for cancer immune escape. *Cells*. 2019;8:558-568. [\[CrossRef\]](#)
 20. Zhang PF, Gao C, Huang XY, et al. Cancer cell-derived exosomal circUHRF1 induces natural killer cell exhaustion and may cause resistance to anti-PD1 therapy in hepatocellular carcinoma. *Mol Cancer*. 2020;19:110. [\[CrossRef\]](#)
 21. Berchem G, Noman MZ, Bosseler M, et al. Hypoxic tumor-derived microvesicles negatively regulate NK cell function by a mechanism involving TGF- β and miR23a transfer. *Oncimmunology*. 2015;5:e1062968. [\[CrossRef\]](#)
 22. Chen J, Song Y, Miao F, et al. PDL1-positive exosomes suppress antitumor immunity by inducing tumor-specific CD8+ T cell exhaustion during metastasis. *Cancer Sci*. 2021;112:3437-3454. [\[CrossRef\]](#)
 23. Poggio M, Hu T, Pai CC, et al. Suppression of Exosomal PD-L1 Induces Systemic Anti-tumor Immunity and Memory. *Cell*. 2019;177:414-427. [\[CrossRef\]](#)
 24. Zheng Y, Xu M, Zeng D, et al. In situ analysis of hepatitis B virus (HBV) antigen and DNA in HBV-induced hepatocellular carcinoma. *Diagn Pathol*. 2022;17:11. [\[CrossRef\]](#)
 25. Fu S, Li N, Zhou PC, Huang Y, Zhou RR, Fan XG. Detection of HBV DNA and antigens in HBSAg-positive patients with primary hepatocellular carcinoma. *Clin Res Hepatol Gastroenterol*. 2017;41:415-423. [\[CrossRef\]](#)
 26. Cammarota A, Zanuso V, Pressiani T, Personeni N, Rimassa L. Assessment and monitoring of response to systemic treatment in advanced hepatocellular carcinoma: current insights. *J Hepatocell Carcinoma*. 2022;9:1011-1027. [\[CrossRef\]](#)
 27. Yi X, Yu S, Bao Y. Alpha-fetoprotein-L3 in hepatocellular carcinoma: a meta-analysis. *Clin Chim Acta*. 2013;425:212-20. [\[CrossRef\]](#)
 28. Tümen D, Heumann P, Gülow K, et al. Pathogenesis and current treatment strategies of hepatocellular carcinoma. *Biomedicines*. 2022;10:3202-3241. [\[CrossRef\]](#)
 29. Umar Garzali İ, Carr B, Ince V, Işık B, Nur Akatlı A, Yılmaz S. Microvascular invasion in hepatocellular carcinoma: some puzzling facets. *Turk J Gastroenterol*. 2024;35:143-149. [\[CrossRef\]](#)
 30. Karaoğullarından Ü, Üsküdar O, Odabaş E, Ak N, Kuran S. Hepatocellular carcinoma in cirrhotic versus noncirrhotic livers: clinicomorphologic findings and prognostic factors. *Turk J Gastroenterol*. 2023;34:262-269. [\[CrossRef\]](#)
 31. Jin AL, Yang YH, Su X, et al. High serum soluble CD155 level predicts poor prognosis and correlates with an immunosuppressive tumor microenvironment in hepatocellular carcinoma. *J Clin Lab Anal*. 2022;36:e24259. [\[CrossRef\]](#)
 32. Okumura G, Iguchi-Manaka A, Murata R, Yamashita-Kanemaru Y, Shibuya A, Shibuya K. Tumor-derived soluble CD155 inhibits DNAM-1-mediated antitumor activity of natural killer cells. *J Exp Med*. 2020;217:1. [\[CrossRef\]](#)
 33. Iguchi-Manaka A, Okumura G, Ichioka E, et al. High expression of soluble CD155 in estrogen receptor-negative breast cancer. *Breast Cancer*. 2020;27:92-99. [\[CrossRef\]](#)
 34. Mashouri L, Yousefi H, Aref AR, Ahadi AM, Molaei F, Alahari SK. Exosomes: composition, biogenesis, and mechanisms in cancer metastasis and drug resistance. *Mol Cancer*. 2019;18:75-89. [\[CrossRef\]](#)
 35. Chen XP, Long X, Jia WL, et al. Viral integration drives multifocal HCC during the occult HBV infection. *J Exp Clin Cancer Res*. 2019;38:261. [\[CrossRef\]](#)
 36. Bertoletti A, Kennedy PTF, Durantel D. HBV infection and HCC: the "dangerous liaisons". *Gut*. 2018;67:787-788. [\[CrossRef\]](#)
 37. Yu X, Zheng Y, Huang R, et al. Restoration of CD3+CD56+ NKT-like cell function by TIGIT blockade in inactive carrier and immune tolerant patients of chronic hepatitis B virus infection. *Eur J Immunol*. 2024;54:e2451046. [\[CrossRef\]](#)
 38. Wang J, Hou H, Mao L, et al. TIGIT signaling pathway regulates natural killer cell function in chronic hepatitis b virus infection. *Front Med (Lausanne)*. 2022;8:816474. [\[CrossRef\]](#)
 39. Luo P, Wu S, Yu Y, et al. Current status and perspective biomarkers in AFP negative HCC: towards screening for and diagnosing hepatocellular carcinoma at an earlier stage. *Pathol Oncol Res*. 2020;26:599-603. [\[CrossRef\]](#)
 40. Wang Y, Deng B. Hepatocellular carcinoma: molecular mechanism, targeted therapy, and biomarkers. *Cancer Metastasis Rev*. 2023;42:629-652. [\[CrossRef\]](#)
 41. Mechref Y, Peng W, Gautam S, et al. Mass spectrometry based biomarkers for early detection of HCC using a glycoproteomic approach. *Adv Cancer Res*. 2023;157:23-56. [\[CrossRef\]](#)
 42. Yu W, Hurler J, Roberts D, et al. Exosome-based liquid biopsies in cancer: opportunities and challenges. *Ann Oncol*. 2021;32:466-477. [\[CrossRef\]](#)
 43. Yu D, Li Y, Wang M, et al. Exosomes as a new frontier of cancer liquid biopsy. *Mol Cancer*. 2022;21:56-89. [\[CrossRef\]](#)
 44. Hu J, Wang E, Liu L, et al. Sorafenib may enhance antitumor efficacy in hepatocellular carcinoma patients by modulating the proportions and functions of natural killer cells. *Invest New Drugs*. 2020;38:1247-1256. [\[CrossRef\]](#)
 45. Xie Q, Hu C, Luo C. The alterations in peripheral lymphocyte subsets predict the efficacy and prognosis of immune checkpoint inhibitors in hepatocellular carcinoma. *J Cancer*. 2023;14:2946-2955. [\[CrossRef\]](#)
 46. Gryziak M, Wozniak K, Kraj L, Rog L, Stec R. The immune landscape of hepatocellular carcinoma-where we are? *Oncol Lett*. 2022;24:410. [\[CrossRef\]](#)
 47. Zhang Q, Bi J, Zheng X, et al. Blockade of the checkpoint receptor TIGIT prevents NK cell exhaustion and elicits potent anti-tumor immunity. *Nat Immunol*. 2018;19:723-732. [\[CrossRef\]](#)
 48. Ashiru O, Boutet P, Fernández-Messina L, et al. Natural killer cell cytotoxicity is suppressed by exposure to the human NKG2D ligand MICA*008 that is shed by tumor cells in exosomes. *Cancer Res*. 2010;70:481-489. [\[CrossRef\]](#)
 49. Chen Y, You F, Jiang L, et al. Gene-modified NK-92MI cells expressing a chimeric CD16-BB- ζ or CD64-BB- ζ receptor exhibit enhanced cancer-killing ability in combination with therapeutic antibody. *Oncotarget*. 2017;8:37128-37139. [\[CrossRef\]](#)
 50. Huang CH, Liao YJ, Fan TH, Chiou TJ, Lin YH, Twu YC. A developed NK-92MI cell line with siglec-7neg phenotype exhibits high and sustainable cytotoxicity against leukemia cells. *Int J Mol Sci*. 2018;19:1073-1087. [\[CrossRef\]](#)